FEBS Letters 581 (2007) 962–966

Anti-angiogenic properties of *myo*-inositol trispyrophosphate *in ovo* and growth reduction of implanted glioma

Gabin Sihn[a,*,1], Thomas Walter[b], Jean-Claude Klein[b], Isabelle Queguiner[a], Hiroshi Iwao[c], Claude Nicolau[d], Jean-Marie Lehn[e], Pierre Corvol[a], Jean-Marie Gasc[a]

[a] *Laboratoire de Pathologie Vasculaire et Endocrinologie Rénale, Inserm U36, Collège de France, 11, place Marcelin Berthelot, 75005 Paris, France*
[b] *Ecole des Mines de Paris, Centre de Morphologie Mathématique, 35, rue St-Honoré, 77305 Fontainebleau, France*
[c] *Osaka City University Medical School, Osaka, Japan*
[d] *Oxyplus, Inc., 200 Boston Avenue, Medford, MA 02155, USA*
[e] *Laboratoire de Chimie Supramoléculaire, ISIS-Université Louis Pasteur, 8, allée Gaspard Monge, BP 70028, 67083 Strasbourg Cedex, France*

Received 21 November 2006; revised 29 January 2007; accepted 30 January 2007

Available online 14 February 2007

Edited by Vladimir Skulachev

Abstract **We investigate here the anti-angiogenic properties of the synthetic compound *myo*-inositol trispyrophosphate (ITPP). By increasing oxy-haemoglobin dissociation, ITPP has the potential to counteract the effects of hypoxia, a critical regulator of angiogenesis and cancer progression. ITPP inhibited angiogenesis of the chorioallantoic membrane (CAM), as analyzed with an original program dedicated to automated quantification of angiogenesis in this model. ITPP also markedly reduced tumor progression and angiogenesis in an experimental model of U87 glioma cell nodules grafted onto the CAM. These results point out the potential of ITPP for the development of a new class of anti-angiogenic and anti-cancer compounds.**

Keywords: Angiogenesis; Allosteric effector; Chorioallantoic membrane; Haemoglobin; Inositol hexakisphosphate; Inositol trispyrophosphate; Partial oxygen pressure; Tumor; Vascular quantification

1. Introduction

Angiogenesis, the main process of blood vessel formation, is a hallmark of tumor progression [1], and anti-angiogenic compounds are extensively studied for anti-cancer therapy [2]. However, angiogenesis involves complex regulatory pathways, and compounds that are currently used in clinical trials, notably blockers of vascular growth factors and inhibitors of their tyrosine kinase receptors, have limited efficacy and exert some secondary effects [3]. Therefore, new strategies are required to sharpen and increase the efficiency of anti-angiogenic therapy.

Myo-inositol trispyrophosphate (ITPP) is a synthetic compound derived from *myo*-inositol hexakisphosphate (IP_6), a natural molecule ubiquitously produced in mammalian cells and previously reported for antioxidant [4] and anticancer [5] properties. Unlike IP_6, ITPP, which bears lower negative charge, is soluble in both aqueous and lower polarity media [6]. It is thus able to cross the red blood cell (RBC) membrane and act as an allosteric effector, increasing the oxygen release from free haemoglobin as well as from whole blood [7]. In contrast, IP_6 must be introduced into the RBC by physical methods in order to increase their oxygen release [8].

It was hypothesized that ITPP, by increasing the partial pressure of oxygen (pO_2) in hypoxic tissues, may act as an anti-angiogenic compound. Indeed, pO_2 is a crucial regulator of angiogenesis: hypoxia is a major activator of blood vessel formation [9,10], while hyperoxia has opposite effects [10]. Human microvascular endothelial cells submitted to hypoxia in the presence of human red blood cells loaded with ITPP do not form capillary tube-like structures and do not express HIF-1 [11]. In this report, we show that ITPP triggers defects in the vascular network of the chick chorioallantoic membrane (CAM) *in ovo*, consistent with an anti-angiogenic effect during physiological angiogenesis. To describe quantitatively the effects observed, we developed a new program that allows automated quantification of several vascular network parameters on angiographic images of the CAM. This original program should prove useful for analysis of pro- or anti-angiogenesis in the model of the CAM as it allows accurate, quick and easy quantification on large series of images. Finally, we report the ability of ITPP to inhibit tumor growth and angiogenesis in an experimental model of human glioma grafted onto the CAM.

2. Materials and methods

Myo-inositol trispyrophosphate (ITPP) was prepared from *myo*-inositol hexakisphosphate (IP_6) as previously described [7,11].

2.1. Chick embryos and cells

Fertilized eggs from White Leghorn chickens were obtained from a commercial breeder (Haas, Kalten House, France). U87 human glioma cells (American Type Culture Collection) were maintained in modified E-MEM (LGC Promochem, France) with 10% FBS.

*Corresponding author. Present address: Max-Delbrück-Center for Molecular Medicine, Robert-Rössle Strasse 10, 13125 Berlin-Buch, Germany. Fax: +49 30 9406 2110.
E-mail address: g.sihn@mdc-berlin.de (G. Sihn).

[1]Gabin Sihn holds a fellowship from the Fondation pour la Recherche Médicale, Paris, France.

Abbreviations: CAM, chorioallantoic membrane; FOV, first order vessel; IP_6, inositol hexakisphosphate; ITPP, inositol trispyrophosphate; pO_2, partial oxygen pressure; SOV, second order vessel; VBR, vessel/background ratio

0014-5793/$32.00
doi:10.1016/j.febslet.2007.01.079

2.2. Chorioallantoic membrane angiogenic assay

The chorioallantoic membrane (CAM) assay was adapted from Celerier et al. [12]. At embryonic day 8 (E8), each CAM received two silicon rings (10 mm-ID) laid onto two areas looking alike for their vascularization. Twenty-five microliters of ITPP hexasodium salt 0.1 M [7] were applied on the first ring, and 25 μl of vehicle (0.15 M NaCl + 2.5 mM $CaCl_2$) on the second one. After 24 h treatment, CAM were either analyzed on angiographic pictures after i.v. injection of FITC-dextran (see details in [13]), or collected for molecular histology.

2.3. Quantification of vascular parameters of the CAM

Quantification was carried out on 1.8×-magnified angiographic images. Automated quantification was performed as follows:

(A) *Vessel segmentation*. After normalizing the dynamic range of the images, a prefiltering step was applied to remove the capillary bed (morphological closing by reconstruction, dynamic filtering [14] and volume leveling [15]). Then, the following threshold scheme was applied: (1) A first (high) threshold was applied on the prefiltered image in order to segment the bright (thick) vessels. (2) The small vessels were extracted from the prefiltered image by means of the top-hat transformation [14], smoothed in their main direction with a Gaussian profile filter [16], and segmented with a second (low) threshold. These results were combined resulting in a binary image representing the vessels.

(B) *Finding the extremities*. Extremities of a binary set coincide with the local maxima of its geodesic distance map [17,18]. However, parasite maxima may exist due to (1) border irregularities and (2) loops in the segmentation result. These two problems have been overcome by (1) removing all local maxima with low dynamic [14] and (2) carrying along a label image while constructing the geodesic distance map, allowing the identification of bifurcations, and therewith the identification of the parasite maxima [18]. This method has been implemented efficiently using FIFO-structures (queues). By the end of this procedure, all endpoints of the vascular tree were obtained, which coincided with the first order vessels [19].

(C) *Calculation of a clean skeleton*. The classical skeleton (set of one pixel wide lines) of the vascular tree was calculated. From this skeleton, we removed all branches with endpoints not coinciding with the ones calculated in section 2.

(D) *Calculation of parameters*. From the segmentation result (A) the ratio of the number of vascular pixels to the number of non vascular pixels (VBR, vessel background ratio) was calculated, reflecting the vascular density. Alternatively, this measure can be calculated for small vessels only (SVBR), in order to avoid the bias induced by large vessels. The extremities (B) gave the number of first order vessels (FOV). With the skeleton (C) the number of bifurcations (three outgoing branches), the number of crossings (four or more outgoing branches), the number of second order vessels (SOV) [19], and the length distribution and total length of the vascular tree were calculated.

2.4. Reliability of the automated quantification

Results obtained by manual observation by three different observers were compared to those of automated quantification. For this comparison, which was made on nine CAMs of a single experiment, the FOV parameter was investigated. Plotting the computed data against those of each observer revealed linear regression curves with scores (R^2) of 0.74 ± 0.02 (Fig. 1B). As well, inter-observer comparisons also led to linear curves with R^2 of 0.82 ± 0.03 (Fig. 1B). Equations of the regression curves are in Fig. 1B.

2.5. Experimental glioma assay

Experimental human glioma assays were performed on the CAM as described by Hagedorn et al. [20]: at E10, a silicon ring was laid onto the CAM, and 3–5 million U87 human glioma cells in 20 µl of medium were deposited after gentle laceration of surface. At E12, embryos bearing size-matching tumors were treated until E14 with 25 µl per day of either ITPP 0.1 M or the vehicle. The effect of ITPP was analyzed on the tumoral growth and vascularization, and appearance of hemorrhages within the tumor.

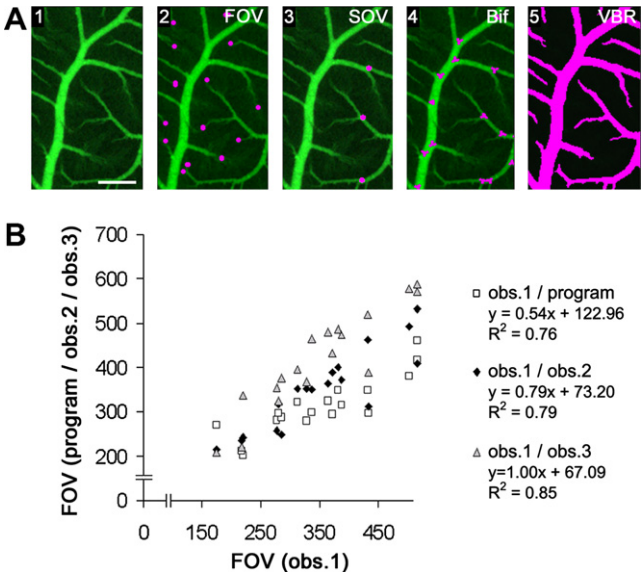

Fig. 1. Automated quantification. (A) Computed analysis of CAM vasculature, allowing, from an angiographic image (inset 1), the quantification of first order vessels (FOV, inset 2), second order vessels (SOV, inset 3) Bifurcations (Bif, inset 4) and vessel/background ratio (VBR, inset 5) parameters, revealed in purple (for details, see Section 2). (B) Plots of computed measurements for the FOV parameter against manual measurements of a first observer (obs. 1). As a comparison, plots of manual measurements of two other observers (obs. 2 and obs. 3) against obs. 1 are shown. The equations of the regression curves obtained for the different plots as well as their correlation scores (R^2) are indicated. Scale bar: 400 µm.

2.6. Histological procedures

Tissues were fixed overnight in 4% paraformaldehyde at 4 °C, dehydrated in graded alcohol, cleared in xylene, embedded in paraffin, and cut into 7 µm-thick sections. Chick blood vessels were labeled with biotinylated *Sambucus Nigra* lectin (SNA-lectin) (1:1000; Vector, Burlingame, CA), with routine signal amplification by ABC Elite (Vector, Burlingame, CA) and diaminobenzidine as chromogen. For quantification of vascular density within the U87 cell nodules, three fields per section of three different sections were analysed for each nodule as follows: images of SNA-lectin-labeled nodules were taken with a Coolsnap digital camera (Roper Scientific, Trenton, NJ), binarized with a threshold determined manually for each image, and quantified for the number of colored pixels with the IPLab software (IPLab, Scanalytics).

2.7. Statistical analysis

For manual and automatic quantification of vascular parameters of the CAM, a non parametric test of Mann and Whitney was used.

3. Results

3.1. Effects of ITPP on the CAM

ITPP at 0.1 M provoked obvious alterations of the CAM vascular tree as soon as after 24 h of treatment. Compared to the controls (Fig. 2A, C), the vascular network appeared disorganized (Fig. 2B, D) as observed on angiographic pictures, notably at the level of the microvascular bed (Fig. 2D vs C).

We evaluated these defects by measuring several parameters of the vascular network with the program described in Section 2, which allows an automated quantification. Thirteen CAM from two series of experiments were analyzed. A treatment with ITPP led to a significant decrease in parameters such as

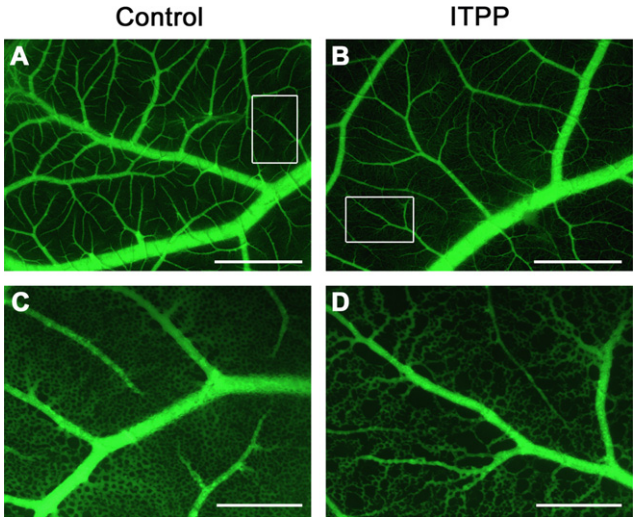

Fig. 2. ITPP defects on CAM vasculature. (A and B) Low magnification angiographic images of CAMs treated with the vehicle (A) or ITPP 0.1 M (B). (C and D) Higher magnifications of the insets of A and B respectively. Scale bars: 2 mm (A and B) and 400 μm (C and D).

number of FOV (13.4%, $P = 0.03$), VBR (33%, $P < 0.001$), number of bifurcations (23%, $P < 0.01$) and total length of the vascular tree (22%, $P < 0.002$) (Fig. 3A–D). The number of SOV was also lowered, although not significantly (7%, $P = 0.1$) (Fig. 3E).

3.2. Effects on experimental glioma

Following an experimental model described previously [20], nodules grown from U87 cells grafted onto the CAM at embryonic day 10 (E10) started to be invaded in their periphery by CAM vessels from E12 onward (onset of treatment). In seven out of eight control nodules (two series of experiments pooled), a large intra-nodular cavity filled with blood developed between E12 and E14 (Fig. 4). In nodules treated with ITPP 0.1 M, these hemorrhages were reduced both in terms of incidence (6 out of 11 nodules) and intensity (Fig. 4).

3.3. ITPP decreased nodule invasion by CAM vessels

Histological analysis was performed on two control and four ITPP-treated nodules. Sections of E14 (2 days of treatment) control nodules showed a highly necrotic core, while the area at the frontline with the CAM was rich in blood vessels of chick origin, as revealed by labeling with SNA-lectin (Fig. 5A). In ITPP-treated nodules, a necrotic core and a vascularized area were also visible (Fig. 5B, C). However, measurements of vascular density in the vascularized area (see specific characteristics of this quantification in Section 2) revealed a significant decrease in ITPP-treated glioma (Fig. 5E, F) compared to controls (Fig. 5D) (28.37 ± 0.77 vs 23.85 ± 0.83, $P < 0.002$; 3 ITPP-treated and two control nodules were analyzed). Thickness of this area also appeared reduced (Fig. 5A vs B, C).

4. Discussion

ITPP has been synthesized as a derivative of IP_6 with increased membrane permeability and the ability to lower Hb affinity for oxygen on free Hb as well as on whole blood [7]. Since pO_2 is an important regulator of angiogenesis, we hypothesized that, by facilitating oxygen availability at physiological pO_2 values, ITPP could act as an anti-angiogenic compound.

In the CAM model, ITPP triggered an apparent disorganization and a decreased vascular density of the vasculature, as ob-

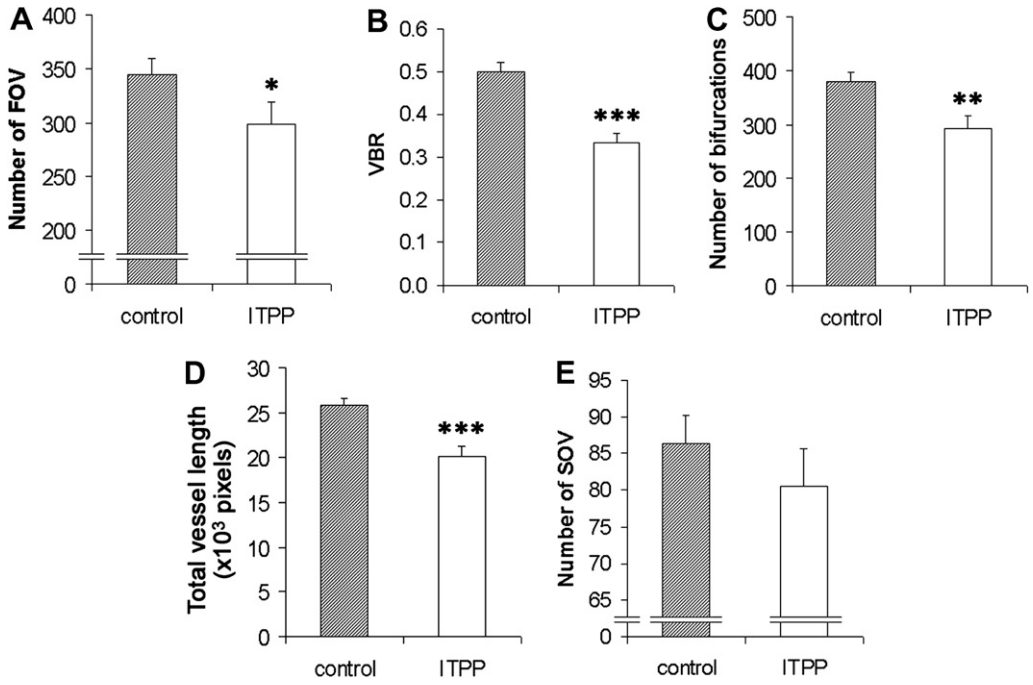

Fig. 3. Quantification of ITPP defects on CAM vasculature. Computed quantification of number of first order vessels (FOV) (A), vessel/background ratio (VBR) (B), number of bifurcations (C), total length of the vascular tree (D) and number of second order vessels (SOV) (E). Values are means ± S.E.M. $^{*}P = 0.03$; $^{**}P = 0.01$; $^{***}P < 0.002$.

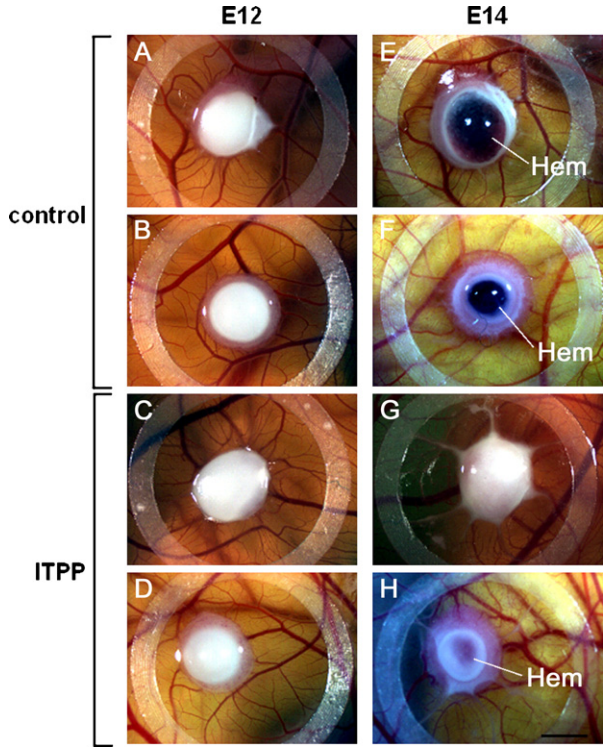

Fig. 4. Effects of ITPP on the development of experimental U87 glioma. U87 cells growing as nodules on CAM treated with vehicle (A, B, E, F) or ITPP 0.1 M (C, D, G, H). (A–D) nodules at E12 (beginning of the treatment). (E–F) same nodules at E14. Hem: hemorrhages. Scale bar: 2 mm.

served visually on low magnification angiographic images, consistent with an anti-angiogenic effect. In order to assess the significance and reproducibility of the effect, architectural parameters of the vascular tree were quantified. Such quantification required automated tools as manual quantification is time-consuming and prone to subjectivity. However, few of the automated methods currently described allow a real automatic and exhaustive description of the vascular network. For this purpose, we developed a computer-based program allowing an easy and fast quantification on large series of images, of several parameters relevant to describe the morphology of the CAM vasculature. The program proved reliable, as: (i) it provided a full intra-assay reproducibility while manual quantification displayed both intra- and inter-observer variability (data not shown), and (ii) plots of the automated against the manual results for the "number of FOV" showed linear regression curves with high correlation scores. All parameters computed by the program were affected, notably concerning the total vessel length, the VBR (which reflects the vascular density), the number of bifurcations and the number of FOV. The number of SOV was less affected than the other parameters, which may reflect the heterogeneity of the vascular tree: the SOV, which correspond to larger and more mature vessels than FOV, may be less prone to remodeling and for this reason less sensitive to the action of ITPP.

The effects observed on the development of experimental tumors grafted onto the CAM were also indicative of anti-angiogenic properties of ITPP. This experimental tumor, in presence of the control solution, showed blood vessel development from E12 and the appearance of necrotic area and hemorrhages at later stages. As early as after 2 days of ITPP treatment, the size of nodules was reduced and less hemorrhages occurred. In addition, there was a decrease in the vascularized area and a reduction in the number of neovessels. These data suggest that ITPP may serve as an anti-tumoral compound, notably acting via inhibition of angiogenesis. In support of this hypothesis, ITPP had no effect on U87 cell proliferation *in vitro* (assessed by both [^{3}H]-thymidine incorporation and MTT assays, data not shown) at concentrations up to at least 0.01 M.

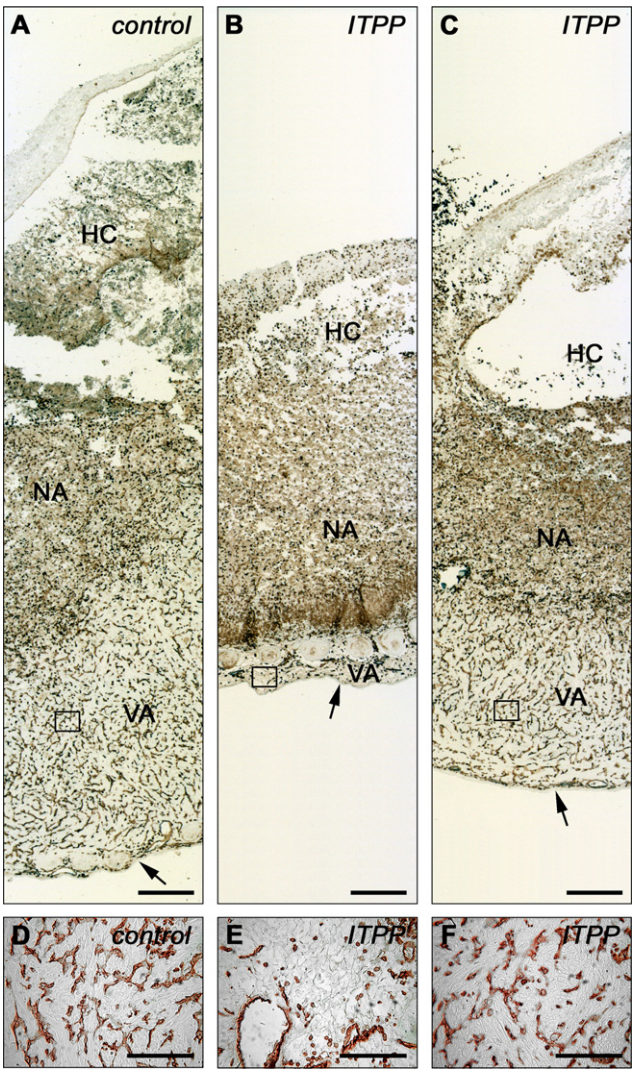

Fig. 5. Histochemical analysis of experimental U87 glioma at E14 after treatment with ITPP. (A–C) transversal sections of a control nodule (A) and two ITPP-treated nodules with strong (B) or moderate (C) responses to treatment, labeled with *Sambucus Nigra* lectin; arrows point the CAM. (D–F) higher magnifications of the insets of A–C respectively. VA, vascularized area; NA, necrotic area; HC, hemorrhagic cavity. Scale bars: 250 μm (A–C) and 100 μm (D–F).

The mechanisms by which ITPP may interfere with angiogenesis remain to be determined. Our hypothesis was that ITPP could counteract hypoxia-induced angiogenesis. In support of this hypothesis, capillary tube formation by endothelial cells is specifically inhibited *in vitro* in presence of ITPP-loaded red blood cells made thus capable to release higher amounts of O_2, while ITPP alone has no effect [11]. In addition, ITPP has no effect on endothelial cell proliferation *in vitro* (see annexe).

However, such a mechanism may not be the only one responsible for the effects of ITPP, notably on the physiological neoangiogenesis of the CAM, studied under room atmosphere (pO_2 around 150 Torr) while ITPP as well as IP_6 are active on haemoglobin for pO_2 values up to 125 Torr [7]. Therefore, other mechanisms of action have to be considered. ITPP actions may be converted intracellularly into IP_6 or other bioactive phosphatidylinositols, as it has been shown for IP_6 itself [5]. In addition, anti-angiogenic properties of IP_6 have been reported [21]. However, no data are currently available about ITPP metabolism *in vivo*. It appears that, when considering the inhibition of angiogenesis by ITPP two main mechanisms should be considered: (1) an indirect one, when ITPP is taken up by RBCs and thus lowers the affinity of hemoglobin for O_2, leading to delivery of higher oxygen amounts under hypoxia, and (2) a direct mechanism, following the uptake of ITPP by cells and its subsequent metabolism within those cells.

Doses used for ITPP treatments were high: 2.5 μmoles applied on a 1 cm^2-surface for the treatments on the CAM and U87 cell nodules. No significant effect of ITPP was observed in the CAM assay with three time-lower doses (0.8 μmoles) (data not shown). Requirement of such high doses for the effect to occur may be explained if the main mechanism of action was via the allosteric regulation of oxygen delivery by the RBCs, which would require ITPP to cross the plasma membranes of these cells. Although its membrane permeability is higher than IP_6, ITPP still remains a polar molecule displaying six negative charges. More permeant compounds with ITPP properties might be interesting to investigate in this respect. Even at the high doses, ITPP did not appear to be toxic for the chick embryo, which is in accordance with the lack of toxicity observed on cell cultures *in vitro* and in mice *in vivo* (unpublished data). Similarly, IP_6 has also been described as non toxic when administered to animals [22,23] and humans [24,25].

In conclusion, we suggest that ITPP may be a compound of interest for anti-cancer strategies, considering its anti-angiogenic properties. Although the mechanisms of action of ITPP are not fully understood, its ability to minimize or remove hypoxia points out to a novel approach for regulating angiogenic processes.

Acknowledgments: We acknowledge Noel Lamande for his involvement in the computed quantification development, and Herve Kempf, and Etienne Larger for their helpful advice. We are grateful to Anais Caillard, Maud Clemessy, Severine Ledoux, Matthieu Lesage, Li Li and Francois Vincent for their general help. This work was supported by INSERM and the Ecole des Mines de Paris. Gabin Sihn holds a doctoral fellowship from the Fondation pour la Recherche Medicale.

Appendix A. Supplementary data

Supplementary data associated with this article can be found, in the online version, at doi:10.1016/j.febslet.2007.01.079.

References

[1] Folkman, J. (1971) Tumor angiogenesis: therapeutic implications. N. Engl. J. Med. 285, 1182–1186.
[2] Jubb, A.M., Oates, A.J., Holden, S. and Koeppen, H. (2006) Predicting benefit from anti-angiogenic agents in malignancy. Nat. Rev. Cancer 6, 626–635.
[3] Jain, R.K., Duda, D.G., Clark, J.W. and Loeffler, J.S. (2006) Lessons from phase III clinical trials on anti-VEGF therapy for cancer. Nat. Clin. Pract. Oncol. 3, 24–40.
[4] Graf, E. and Eaton, J.W. (1990) Antioxidant functions of phytic acid. Free Radic. Biol. Med. 8, 61–69.
[5] Vucenik, I. and Shamsuddin, A.M. (2003) Cancer inhibition by inositol hexaphosphate (IP6) and inositol: from laboratory to clinic. J. Nutr. 133, 3778S–3784S.
[6] Vincent, S.P., Lehn, J.M., Lazarte, J. and Nicolau, C. (2002) Transport of the highly charged myo-inositol hexakisphosphate molecule across the red blood cell membrane: a phase transfer and biological study. Bioorg. Med. Chem. 10, 2825–2834.
[7] Fylaktakidou, K.C., Lehn, J.M., Greferath, R. and Nicolau, C. (2005) Inositol tripyrophosphate: a new membrane permeant allosteric effector of haemoglobin. Bioorg. Med. Chem. Lett. 15, 1605–1608.
[8] Nicolau, C., Ropars, C. and Teisseire, B. (1986) Short and long term physiological effects of improved oxygen transport by red blood cells containing inositol hexaphosphate in: Phytic Acid (Graf, E., Ed.), pp. 265–290, Pilatus Press, Minneapolis, MN.
[9] Pouyssegur, J., Dayan, F. and Mazure, N.M. (2006) Hypoxia signalling in cancer and approaches to enforce tumour regression. Nature 441, 437–443.
[10] Strick, D.M., Waycaster, R.L., Montani, J.P., Gay, W.J. and Adair, T.H. (1991) Morphometric measurements of chorioallantoic membrane vascularity: effects of hypoxia and hyperoxia. Am. J. Physiol. 260, H1385–H1389.
[11] Kieda, C., Greferath, R., Crola da Silva, C., Fylaktakidou, K.C., Lehn, J.M. and Nicolau, C. (2006) Suppression of hypoxia-induced HIF-1alpha and of angiogenesis in endothelial cells by myo-inositol trispyrophosphate-treated erythrocytes. Proc. Natl. Acad. Sci. USA 103, 15576–15581.
[12] Celerier, J., Cruz, A., Lamande, N., Gasc, J.M. and Corvol, P. (2002) Angiotensinogen and its cleaved derivatives inhibit angiogenesis. Hypertension 39, 224–228.
[13] Larger, E., Marre, M., Corvol, P. and Gasc, J.M. (2004) Hyperglycemia-induced defects in angiogenesis in the chicken chorioallantoic membrane model. Diabetes 53, 752–761.
[14] Soille, P. (1999) Morphological Image Analysis: Principles and Applications, Springer, Berlin, New York, p. 316.
[15] Vachier, C. (1995) Extraction de caractéristiques, segmentation d'image et morphologie mathématique. Ecole Nationale Supérieure des Mines de Paris, Paris.
[16] Chaudhuri, S., Chatterjee, S., Katz, N., Nelson, M. and Goldbaum, M. (1989) Detection of blood vessels in retinal images using two-dimensional matched filters. IEEE Trans. Med. Imaging 8, 263–269.
[17] Serra, J. (2002) Morphological descriptions using three-dimensional wavefronts. Image Anal. Stereol. 21, S13–S21.
[18] Angulo, J. and Matou, S. (2006) Application of mathematical morphology to the quantification of *in vitro* endothelial cell organization into tubular-like structures. Cell Mol. Biol.
[19] DeFouw, D.O., Rizzo, V.J., Steinfeld, R. and Feinberg, R.N. (1989) Mapping of the microcirculation in the chick chorioallantoic membrane during normal angiogenesis. Microvasc. Res. 38, 136–147.
[20] Hagedorn, M., Javerzat, S., Gilges, D., Meyre, A., de Lafarge, B., Eichmann, A. and Bikfalvi, A. (2005) Accessing key steps of human tumor progression *in vivo* by using an avian embryo model. Proc. Natl. Acad. Sci. USA 102, 1643–1648, (Epub 2005 January 21).
[21] Vucenik, I., Passaniti, A., Vitolo, M.I., Tantivejkul, K., Eggleton, P. and Shamsuddin, A.M. (2004) Anti-angiogenic activity of inositol hexaphosphate (IP6). Carcinogenesis 25, 2115–2123.
[22] Ullah, A. and Shamsuddin, A.M. (1990) Dose-dependent inhibition of large intestinal cancer by inositol hexaphosphate in F344 rats. Carcinogenesis 11, 2219–2222.
[23] Dong, Z., Huang, C. and Ma, W.Y. (1999) PI-3 kinase in signal transduction, cell transformation, and as a target for chemoprevention of cancer. Anticancer Res. 19, 3743–3747.
[24] Henneman, P.H., Benedict, P.H., Forbes, A.P. and Dudley, H.R. (1958) Idiopathic hypercaicuria. N. Engl. J. Med. 259, 802–807.
[25] Druzijanic, N., Juricic, J., Perko, Z. and Kraljevic, D. (2002) IP-6 & inositol: adjuvant to chemotherapy of colon cancer. A pilot clinical trial. Rev. Oncologia, 171.